

Status Report

SIMULATION OF MICELLAR-POLYMER FLOODING IN A BARRIER ISLAND SYSTEM

Project BE1, Milestone 2, FY89

By Ming-Ming Chang

Work performed for the
U. S. Department of Energy
Under Cooperative Agreement
DE-FC22-83FE60149

Edith Allison, Project Manager
Bartlesville Project Office
U. S. Department of Energy

DISCLAIMER

This report was prepared as an account of work sponsored by an agency of the United States Government. Neither the United States Government nor any agency thereof, nor any of their employees, makes any warranty, express or implied, or assumes any legal liability or responsibility for the accuracy, completeness, or usefulness of any information, apparatus, product, or process disclosed, or represents that its use would not infringe privately owned rights. Reference herein to any specific commercial product, process, or service by trade name, trademark, manufacturer, or otherwise, does not necessarily constitute or imply its endorsement, recommendation, or favoring by the United States Government or any agency thereof. The views and opinions of authors expressed herein do not necessarily state or reflect those of the United States Government or any agency thereof.

IIT Research Institute
NATIONAL INSTITUTE FOR PETROLEUM AND ENERGY RESEARCH
P. O. Box 2128
Bartlesville, Oklahoma 74005
(918) 336-2400

TABLE OF CONTENTS

	<u>Page</u>
Abstract.....	1
Introduction.....	1
Barrier island deposition system -- Bell Creek field.....	2
UTCHEM simulator and its modification.....	3
Reservoir simulation.....	6
Simulation results.....	8
Summary.....	9
References.....	9

TABLES

1. Formation properties in the reservoir model of a barrier island deposystem.....	12
2. Langmuir adsorption parameters of surfactant and polymer on clay.....	12
3. Cation exchange properties for various types of clay.....	12
4. Micellar-polymer flooding simulation parameters.....	13
5. Injected compositions -- micellar-polymer flooding simulation.....	14
6. Injection/production rates in model study based on production rates of well P-10 in Unit 'A'.....	15
7. Simulation results of micellar-polymer flooding in barrier island deposystem.....	17

ILLUSTRATIONS

1. Three-dimensional reservoir model for barrier-island deposystem..	18
2. Oil recovery and oil cut from a clay-free barrier island reservoir.....	18
3. Oil recovery and oil cut from a reservoir containing 0.5% kaolinite in barrier island sand.....	19
4. Oil recovery and oil cut from a reservoir containing 2.5% kaolinite in barrier island sand.....	19

ILLUSTRATIONS -- Continued

Page

5. Oil recovery and oil cut from a reservoir containing 5% kaolinite in barrier island sand.....	20
6. Oil recovery and oil cut from a reservoir containing 7.5% kaolinite in barrier island sand.....	20
7. Oil recovery from a barrier island reservoir containing various amount of clay.....	21
8. Surfactant profile in aqueous phase from a barrier island reservoir containing various amount of clay.....	21
9. Polymer profile from a barrier island reservoir containing various amount of clay.....	22
10. Chloride and calcium profile from a barrier island reservoir containing 0.5% kaolinite in barrier island sand.....	22
11. Profile of effective salinity from a barrier island reservoir containing 0.5% kaolinite in barrier island sand.....	23
12. Effect of preflush period on oil recovery from a reservoir containing 0.5% kaolinite in barrier island sand.....	23
13. Effect of preflush period on oil recovery from a reservoir containing 2.5% kaolinite in barrier island sand.....	24

SIMULATION OF MICELLAR-POLYMER FLOODING IN A BARRIER ISLAND SYSTEM

By Ming-Ming Chang

ABSTRACT

Numerical simulations are being conducted to study the effects of clay and other formation heterogeneities on chemically enhanced oil recovery processes in a barrier island deposystem. Formation properties obtained from Unit 'A' in Bell Creek (MT) field were used to construct a reservoir model for the study. The simulator UTCHEM was modified to accept different cation exchange and adsorption parameters in each reservoir grid block for a heterogeneous distribution of clay type and amount.

Different types and amounts of clay showed a significant effect on the incremental oil recovery by micellar-polymer flooding. For a typical range of clay content (0.5 to 7.5% in the barrier sand) found in a barrier island deposystem, the increase of clay could reduce the oil recovery after waterflood from 35 to 15%. Clay retained the surfactant and polymer through adsorption, ion exchange, and precipitation. Simulation results showed that an increase of preflush period improved the oil recovery through the increase of effective salinity in the water phase.

INTRODUCTION

The objective of this study is to investigate, by use of numerical simulation, the effects of formation heterogeneities found in barrier island deposystems on chemical flooding processes. Barrier island depositional systems comprise at least six giant oil fields in North America.¹ Therefore, there is considerable economic merit in understanding geological heterogeneities and their effects in exploiting shallow marine barrier island deposits. The barrier island oil field selected for analysis is Unit 'A' of Bell Creek field on the northeastern flank of the Powder River Basin in Montana.

Bell Creek field² was discovered in 1967 and produced through pressure depletion until a linedrive waterflood pattern was initiated in the field in

1970. Since 1976, two chemical tertiary recovery pilot projects have been completed within Unit 'A'. The northern pilot was only marginally successful because of unanticipated geological complexity. The southern pilot implemented through the DOE tertiary oil incentive program (TIP) was more successful. Different results from the two pilots were speculated to be due to the effect of geological heterogeneities on the micellar-polymer flooding process.

Major geological heterogeneities encountered in Bell Creek field and their influence on primary and secondary production have been previously discussed.³ Preliminary production analysis and numerical simulation runs were performed for tertiary production in the TIP area within Unit 'A', Bell Creek field.⁴ EOR simulation work performed⁵ during fiscal year 1988 included history matching of results of micellar-polymer coreflood experiments with field production from a five-spot pattern of producer P-10 in Unit 'A' using a chemical flooding simulator, UTCHEM. This history matching provided the necessary parameters required to study micellar-polymer flooding in a barrier island deposition system using UTCHEM.

Previous studies about effects of reservoir heterogeneity and flooding design on chemically enhanced oil recovery include salinity gradient,⁶ reservoir crossflow,⁶⁻⁷ fluid phase behavior,⁸ and surfactant concentration and slug size.^{6,8} The clay adsorption and cation exchange phenomena were recognized as important factors in the success of micellar-polymer flooding; however, only a limited amount of work^{7,9} has been done in this area. Since the type and amount of clay vary from facies to facies and from area to area in barrier island deposystems, the study of clay effect on chemical EOR applications in barrier island reservoirs becomes important.

BARRIER ISLAND DEPOSITION SYSTEM -- BELL CREEK FIELD

Barrier islands and valley fills are two major sandstones which comprise the Lower Cretaceous Muddy formation, from which the oil of Unit 'A' in Bell Creek field¹⁰ was produced. Barrier island sandstones may be immediately overlaid by valley fill sandstones which are very fine mean grain size (75 to 125 microns) and contain abundant clay matrix. There are two scales of valley incisions into the best productive barrier island sandstones: a narrow, steep, deep type and a broad type with only moderate relief.

Total thickness of the Muddy formation varies from 42 to 49 ft in one cross section of Unit 'A'. The slight increase of barrier thickness is inversely proportional to total valley thickness. The thickness of the barrier island sandstone varies with an average of about 20 ft and a maximum observed development of 32 ft. The average thickness of valley fill sandstones overlying the barrier sandstone is 7 to 8 ft. The top part of the Muddy formation is developed predominantly as silty and clayey valley fill facies.

Major productive facies within the barrier island sandstones are foreshore and shoreface which are often underlain and overlain by backbarrier (washover) facies. Foreshore and shoreface (especially upper shoreface) facies have much better preservation potential, and they comprise most of the producing barrier island sandstone interval. More than one cycle of vertical stacking of foreshore, upper shoreface, middle shoreface, and lower shoreface facies could be found in barrier island deposystems.

In barrier island sandstones, kaolinite and illite predominate and range from less than 1 to 15%, whereas only trace amounts of smectite (or montmorillonite) are present.¹⁰ Smectite and kaolinite occur commonly in valley fill sandstones and siltstones. Changes in the percentage of total clay generally reflect permeability trends and indicate changes in depositional facies. For example, low permeability is found in clay-rich facies such as lagoonal and lower shoreface facies, and high permeability is found in clay-clean rocks such as upper/middle shoreface and foreshore facies.

UTCHEM SIMULATOR AND ITS MODIFICATION

Description of UTCHEM Simulator

A three-dimensional chemical flood simulator, UTCHEM^{11,12} developed by the Department of Petroleum Engineering at the University of Texas at Austin, was used in this study.

UTCHEM is an isothermal, slightly compressible, multicomponent, three-phase chemical flood compositional simulator. In the simulator, the material balance equations are solved for as many as 19 components. These components may form up to three phases: aqueous, oleic, and microemulsion, depending on relative amounts and effective salinity of the phase environment.

The basic equations describing multicomponent, multiphase flow in porous media are species conservation equations and an overall mass continuity equation. The continuity equation was combined with Darcy's law to obtain the pressure equation. The pressure equation and the (n-1) or 18 material conservation equations were taken as basic independent governing equations for the model formulation.

The solution scheme used is analogous to the implicit pressure, explicit saturation formulation. First, the pressure equation is solved implicitly for phase pressures and velocities using explicit dating of saturation- dependent terms. Then, conservation equations are solved explicitly for total concentrations. Phase concentrations and saturations are determined by flash calculations.

In addition to simulating micellar-polymer flooding, UTCHEM can be used to model tracer flow, in situ gelation, and the high pH flooding process. The major physical phenomena modeled in UTCHEM are phase behavior, phase density, phase viscosity, dispersion, adsorption, cation exchange, dilution effect, interfacial tension, relative permeability, capillary pressure, capillary phase trapping, alcohol partitioning, and polymer properties. The components modeled in the simulator are water, oil, surfactant, polymer, anions, divalent cations, cosurfactant 1, cosurfactant 2, water tracer, partitioning tracer, oil tracer, sodium dichromate, thiourea, trivalent chromium, gel, hydrogen, carbon, and organic acid species.

Adsorption and Cation Exchange Relationships

Clay affects chemical EOR processes through adsorption and cation exchange phenomena. The surfactant and polymer consumed through adsorption on clay will reduce their effectiveness in both lowering the interfacial tension and improving the mobility ratio. The calcium cation released from clay in an ion exchange reaction will precipitate surfactant into the oil phase. The adsorption and cation exchange relationship are defined in UTCHEM as follows:

1. Adsorption. Langmuir type adsorption isotherms of the form¹³

$$\hat{C}_k = \frac{a(K) K_k}{1 + b(K) C_k} \quad (1)$$

are assumed for surfactant and polymer (components $k = 3, 4$), respectively. Where \hat{C}_k , C_k are concentrations of component K in rock and aqueous phases, respectively; $a(K)$ and $b(K)$ are Langmuir adsorption parameters. Surfactant adsorption coefficient $a(3)$ can depend linearly on salinity:

$$a(3) = a(31) + a(32) * CSE \quad (2)$$

where CSE is effective salinity. The parameters $a(31)$, $a(32)$, $a(4)$, $b(3)$, and $b(4)$ are determined experimentally.

2. Cation Exchange

Hirasaki's cation exchange model¹⁴ is used in UTCHEM. This model can be expressed as:

$$\frac{(\hat{C}_{Na})^2}{C_{Ca}} = B_C Q \frac{(C_{Na})^2}{C_{Ca}} \quad \text{for clay} \quad (3)$$

and

$$\frac{(C_{Na}^S)^2}{C_{Ca}^S} = B_S C_S \frac{(C_{Na})^2}{C_{Ca}} \quad \text{for surfactant} \quad (4)$$

where Q is cation exchange capacity (CEC), C is the cation concentration in the aqueous phase, C_S is the surfactant concentration in the aqueous phase, \hat{C} and C^S are amounts of cation adsorbed on clay and surfactant, respectively, and B is an experimentally determined equilibrium constant.

Model Modifications

UTCHEM version 3.2 assumes a single type of clay and a homogeneous distribution of clay in the reservoir, which is seldom the case in reality. Thus, UTCHEM was modified so that different types and various amounts of clay could be considered for adsorption and cation exchange phenomena in each reservoir grid block. Different adsorption parameters, $a(31)$, $a(32)$, $b(3)$, $a(4)$, and $b(4)$, can be assigned to different reservoir blocks according to the

clay distribution. Cation exchange parameters such as CEC, exchange equilibrium constants for clay and surfactant can also be assigned separately to each grid block based on the type and amount of clay.

UTCHEM was also modified to accept a heterogeneous distribution of initial salinity, or initial concentrations of chloride and calcium ions, in the reservoir model.

These modifications to UTCHEM allow users to study how the areal or vertical distribution of clay or salinity affect the success of chemical EOR processes in different reservoirs including barrier island deposystems.

RESERVOIR SIMULATION

Typical reservoir properties in barrier island deposystems were constructed to establish a reservoir model for chemical EOR simulation. Laboratory studies of adsorption and cation exchange for various types of clay described in the literature were used to set up cation exchange and adsorption parameters in UTCHEM.

Numerical Reservoir Model

Union Oil Company's Uniflood™ micellar-polymer flood process² was simulated in a quarter of a 20-acre five-spot field pattern that contained typical reservoir heterogeneities found in barrier island deposystems. A layer of valley fill sandstone was assumed to overlay the barrier island sandstone. Figure 1 shows this three-dimensional reservoir model dimensioned at 6x6x3 with a producer located at one corner and an injector at the opposite corner. This three-layer model has pay thicknesses of 7, 10, and 10 ft representing valley fill, foreshore/upper shoreface, and middle/lower shoreface facies, respectively. Characteristic ratios of vertical to horizontal permeability (k_v/k_h) analyzed from well 26-7 were used in the model: 0.5 for valley fills which overlay productive barrier island facies that have a (k_v/k_h) ratio of about 0.7 for middle shoreface and about 1.0 for foreshore faces. The corresponding layer properties such as porosity, permeability, and types and amounts of clay are listed in table 1.

The amounts of clay were varied in simulation grid blocks to study the effect on micellar-polymer flooding. The clay amount was varied to 15%

montmorillonite in the top valley fill layer, 7.5% total kaolinite and illite in the middle layer (foreshore/upper shoreface facies), and 7.5% total kaolinite and illite plus 1.5% montmorillonite in the bottom layer (middle/lower shoreface facies).¹¹ An average residual oil saturation of 33% after waterflooding found in Unit 'A' of Bell creek field was assumed in all three layers.

Adsorption and Cation Exchange Model

Table 2 shows experimentally measured parameters in a Langmuir type adsorption isotherm for various types of clay.¹⁵⁻¹⁸ Montmorillonite appears to have the highest adsorption capability to both surfactants and polymers. These adsorption parameters (a(31), a(32), and a(4)), which were determined from laboratory tests on clay, are assumed to be extended to clay sand by multiplying them by the percentage of clay within the sandstone.

Table 3 shows the CEC and exchange equilibrium constants between sodium and calcium cations found in the literature^{14,19-20} for various types of clay. Compared to that of other types of clay, montmorillonite has a much higher CEC, montmorillonite is the most important type of clay to consider in replacing calcium cations on clay by sodium cations. As shown in table 3, cation exchange equilibrium constants are about the same for different types of clay. Laboratory-determined sodium-calcium exchange equilibrium constants on surfactants range from 0.2 to 0.45.

Other Input Parameters

Physical property input parameters are given in table 4. These values were used in history matching the production from well P-10. They are acceptable for simulating micellar-polymer flooding in a barrier island deposystem.

Compositions of slugs injected in the TIP of Bell Creek field are given in table 5. These slug compositions were used in the following sensitivity simulation runs. The injection-production scheme, based on production rates from well P-10, was used in the model. Table 6 shows this injection/production scheme.

SIMULATION RESULTS

Micellar-polymer flooding in a barrier island system was simulated at five levels of clay content, including a case of a clay-free reservoir for comparison. Table 7 shows the simulation results and clay types/contents assigned to three layers in each computer run. The adsorption of surfactant and polymer increases with the amount of clay in the reservoir rock. Because of the adsorption of surfactant and polymer on clay, the oil recovery after waterflood decreases from 38% in clay-free reservoirs, to 35% in low-clay reservoirs, and down to 15% in clay-abundant barrier island reservoirs. Figures 2 through 6 show the cumulative oil recovery and oil cut with injected pore volumes for various clay contents. Earlier oil production is due to the changes in effective salinity as a result of ion exchange. A comparison of cumulative oil recoveries from reservoirs containing various amounts of clay is shown in figure 7.

Figure 8 shows produced surfactant concentration profiles from systems with varying amounts of clay. As the clay content increases, the amount of surfactant retention increases, and therefore the produced concentration of surfactant decreases. For the highest amount of clay system studied, only a slight amount of surfactant was produced. This indicates that most of the surfactant is retained and results in a significant reduction of incremental oil recovery. A produced polymer profile in weight percentage from reservoirs containing various amounts of clay is shown in figure 9. Again, the polymer adsorption increases with the clay content of the reservoir rock. Compared to the surfactant profile, however, a significant amount of polymer is still produced from the reservoir of high clay content because of continuous injection of the polymer slug into the reservoir and the low polymer consumption rate. The surfactant and polymer slugs break through right after the produced oil bank at about 0.6 PV of injected fluid.

Production profiles for chloride and calcium ions from a low-clay reservoir are given in figure 10. The calcium ion concentration decreases as the oil cut increases then returns back to its original concentration, 0.0014 M (or meq/mL).

A detailed analysis of the calcium effect on oil recovery determined by a modeling study is underway. The chloride concentration keeps decreasing after the breakthrough of the oil bank because the injected concentration, 0.01667 M, is less than the original concentration, 0.06581 M, in the reservoir.

Note that the simulated micellar-polymer flood failed to reach the optimum range of effective salinity, 0.09 to 0.11 M, assumed in the model. The optimum range of effective salinity is a range of salinities where a third surfactant-rich microemulsion phase was formed. This environment is called the type III phase where all interfacial tensions are the lowest. Figure 11 shows one example of an effective salinity profile from the simulation. These processes stay at the type II(-) phase and never reach the type III phase. The preflush period was then increased from 109 to 183 and 274 days, respectively, to study their effects on oil recovery. Figures 12 and 13 show comparisons of fractional oil recovery at three preflush periods for barrier island reservoirs of two clay contents, respectively. As shown in the figures, more oil is recovered when a preflush is increased from 109 to 183 days, whereas ultimate oil recovery decreases slightly when a preflush is increased from 183 to 274 days. The reason behind this observation is being investigated.

SUMMARY

1. UTCHEM was modified to accept heterogeneous distributions of salinity, adsorption, and cation exchange parameters for studying clay effects on micellar-polymer flooding.

2. Varying types and amounts of clay show significant effects on incremental oil recovery from micellar-polymer flooding. For a typical range of clay content found in barrier island deposystems, an increase in clay from 0 to 15% could reduce oil recovery from 35 to 15%.

3. Clay retains surfactants and polymers through adsorption, precipitation, phase behavior changes, and ion exchange. An increase in the preflush period would increase the oil recovery in this studied case.

REFERENCES

1. Moody, J. A. Giant Oil Fields of North America. Geology of Giant Petroleum Fields, M. T. Halbouty (ed.) AAPG, Memoir 14, 1970.

2. Hartshorne, J. M. Micellar/Polymer Flood Shows Success in Bell Creek Field. Pres. at the 1984 SPE Ann. Tech. Conf. at Houston, Sept. 16-19. SPE paper No. 13122.
3. Sharma, B., M. M. Honarpour, M. J. Szpakiewicz, and R. A. Schatzinger. Critical Heterogeneities in a Barrier Island Deposit and Their Influence on Primary Waterflood and Chemical EOR Operations. Pres. at the 1987 SPE Ann. Tech. Conf. at Dallas, Sept. 27-30. SPE paper No. 16749.
4. Honarpour, M. M., M. J. Szpakiewicz, R. A. Schatzinger, L. Tomutsa, H. B. Carroll, Jr., and R. W. Tillman. Integrated Geological/Engineering Model for Barrier Island Deposits in Bell Creek Field, Montana. Pres. at 1988 SPE/DOE EOR Symp., Tulsa, April 17-20. SPE/DOE paper No. 17366.
5. Honarpour, M. M. Integrated Reservoir Assessment and Characterization. Department of Energy Report No. NIPER-390, 1989.
6. Gupta, A. D. et al. Effects of Reservoir Heterogeneity on Chemically Enhanced Oil Recovery. SPE Reservoir Engineering, May 1988, pp. 479-488.
7. Saad, N. and G. A. Pope. Simulation of Big Muddy Surfactant Pilot. SPE Reservoir Engineering, Feb, 1989, pp. 24-34.
8. Pope, G. A., B. Wang, and K. Tsaur. A Sensitivity Study of Micellar/Polymer Flooding. Soc. Pet. Eng. J., Dec. 1979, pp. 357-368.
9. Somerton, W. H. and C. J. Radke. Role of Clays in the Enhanced Recovery of Petroleum. Pres. at 1980 SPE/DOE EOR Symp., Tulsa. SPE/DOE paper 8845.
10. Sharma, B. Verification of Geological/Engineering Model in Waterflood Areas. Department of Energy Report No. NIPER 286. 1988.
11. Camilleri, D. Description of an Improved Compositional Micellar/Polymer Simulator. SPE Reservoir Engineering, Nov. 1987, pp. 427-432.
12. Pope, G. A. Mobility Control and Scaleup for Chemical Flooding. Department of Energy Report No. DE85000149, 1986.
13. Hong, C. H. Development of a Two-Dimensional Micellar/Polymer Simulator. Ph.D. Dissertation, Univ. of Texas, 1982.
14. Hirasaki, G. J. Ion Exchange With Clays in the Presence of Surfactant. Soc. Pet. Eng. J., Apr. 1982, pp. 181-192.
15. Hower, W. F. Adsorption of surfactants on Montmorillonite. Core and Clay Minerals, v. 18, 1970, pp. 97-105.
16. Figdore, P. E. Adsorption of Surfactants on Kaolinite: NaCl versus CaCl_2 Salt Effects. J. Colloid and Interface Science, v. 87, No. 2, June 1982, pp. 500-517.

17. Shah, D. L. and R. S. Schechter. Improved Oil Recovery by Surfactant and Polymer Flooding. Academic Press, N.Y., 1977, pp. 522-527.

18. Siffert, B. and Y. Bocquet. Polyacrylamide Adsorption onto Kaolinite in the Presence of Sodium Dodecylbenzenesulfonate in Saline. Colloids and Surfaces, v. II, 1984, pp. 137-143.

19. Hill, H. J. and L. W. Lake. Cation Exchange in Chemical Flooding: Part 3-Experimental. Soc. Pet. Eng. J., Dec. 1978, pp. 445-456.

20. Smith, F. W. Ion-Exchange Conditioning of Sandstones for Chemical Flooding. J. Pet. Tech., June 1978, pp. 959-968.

TABLE 1. - Formation properties in the reservoir model of a barrier island deposystem

Layer	Porosity, %	k_h , md	k_v , md	Montmorillonite, %	Illite and kaolinite, %
A	23	100	50	10	3
B	31	2,000	2,000	0	5
C	28	1,000	700	1	5

TABLE 2. - Langmuir adsorption parameters of surfactant and polymer on clay

Clay	Surfactant			Polymer	
	a(31)	a(32)	b(3)	a(4)	b(4)
Montmorillonite	362	1.8	135	434	135
Kaolinite	7.7	1.8	135	25	135
Illinite	--	--	--	64	135

TABLE 3. - Cation exchange properties for various types of clay

	Cation exchange capacity, meq/100 g	B_C , Exchange equilibrium constant
Montmorillonite	80 - 150	0.15
Kaolinite	3 - 15	0.25 - 0.4
Illite	16 - 40	--
Chlorite	10 - 40	~0.75

TABLE 4. - Micellar-polymer flooding simulation parameters

C_2^*PLC	0.0	T_{32}	-0.903	Ap_1	30
C_2^*PRC	1.0	S_{1rw}	0.4	Ap_2	300
C_{3min}	0.0001	S_{2rw}	0.35	Ap_3	2000
m_{AO}	0.001	S_{3rw}	0.35	β_p	2.0
C_{AO}	0.1	k°_{r1w}	0.08	C_{SE1}	0.01
m_{A1}	0.191	k°_{r2w}	1.0	S_p	-0.65
C_{A1}	0.05	k°_{r3w}	0.7	γ_c	4.0
m_{A2}	0.363	e_{1w}	1.7	$\gamma_{1/2}$	13.0
C_{A2}	0.1	e_{2w}	1.12	P_{α}	1.645
β_6	0.8	e_{3w}	1.5	ϕ_{4eff}/ϕ	0.8
β_7	0.0	S_{1rc}	0.0	b_{rk}	1000
C_{SEL7}	0.09	S_{2rc}	0.0	C_{rk}	0.0186
C_{SEU7}	0.11	S_{3rc}	0.0	C_{pc}	9.0
K^O_w	0.56	k^1_{r1c}	1.0	η_{pc}	2
K^S_w	10.00	k^O_{r2c}	1.0	D	0.0
G_{11}	13.0	k^a_{r3c}	1.0	α_L	0.05
G_{12}	-14.0	e_{1c}	1.7	α_T	0.0
G_{13}	0.0221	e_{2c}	1.12		
G_{21}	13.5	e_{3c}	0.48		
G_{22}	14.0	μ_1	0.63		
G_{23}	0.0221	μ_2	4.8		
$\log(\sigma_{wo})$	1.3	α_1	4.0		
T_{11}	-0.329	α_2	5.0		
T_{12}	-0.778	α_3	-30.0		
T_{21}	-0.431	α_4	0.9		
T_{22}	1.220	α_5	0.7		
T_{31}	-0.411				

TABLE 5. - Injected compositions -- micellar-polymer flooding simulation

	Preflush	Soluble oil	Micellar water	Polymer phase I
Water, volume fraction	1.000	0.04845	0.9962	1.0000
Oil, ¹ volume fraction	0.000	0.67700	0.0000	0.0000
Surfactant, ² volume fraction	0.000	0.25517	0.0038	0.0000
Polymer, ³ wt %	0.000	0.00000	0.0000	⁵ 0.1250
Anions, meq/mL	0.183	0.01667	0.0167	0.0167
Calcium, meq/mL	0.000	0.00000	0.0000	0.0000
Co-solvent, ⁴ volume fraction	0.000	0.01938	0.0000	0.0000

¹ Bell Creek crude oil.

² Mostly Stepan Petrostep™ 465.

³ Liquid Naflo™ 550.

⁴ Butyl Cellosolve.

⁵ Phase II = 0.1150

III = 0.0975

IV = 0.0850

V = 0.0750

VI = 0.0600

VII = 0.0400

VIII = 0.0250

M = 0.0050

TABLE 6. - Injection/production rates in model study based on production rates of well P-10 in Unit 'A'

	Time t, days	D _t , days	Dt _D , PV	Injection/production rates, ft ³ /d
Preflush	109	109	0.0699	1,002
Micellar water	121	12	0.0077	1,002
Micellar slug	146	25	0.0160	1,002
Micellar water	170	24	0.0154	1,002
Micellar slug	201	31	0.0093	468
Micellar water	245	44	0.0132	468
Polymer drive:				
Phase I	280	35	0.0105	468
Phase I	348	68	0.0281	648
Phase II	401	53	0.0219	648
Phase II	417	16	0.0144	1,407
Phase III	462	45	0.0404	1,407
Phase III	588	126	0.1010	1,252
Phase IV	645	57	0.0457	1,252
Phase IV	773	128	0.0893	1,093
Phase V	828	55	0.0384	1,093
Phase V	999	171	0.1062	973
Phase VII ¹	1,102	103	0.0640	973

¹ C-6 Under polymer drive Phase VII.

TABLE 6. - Injection/production rates in model study based on production rates of well P-10 in Unit 'A'-- Continued

	Time t, days	D _t , days	Dt _D , PV	Injection/production rates, ft ³ /d
Polymer Drive:				
Phase VII ²	1118	16	0.0099	973
Phase VII	1133	15	0.0106	973
Phase VII	1178	45	0.0301	973
Phase VII ³	1194	16	0.0107	1102
Phase VII ³	1209	15	0.0100	1102
Phase VIII ⁴	1224	15	0.0100	1046
Phase VIII ⁴	1270	46	0.0319	1046
Phase VIII ⁵	1287	17	0.0117	1086
Phase VIII ⁵	1302	15	0.0067	1086
Phase VIII	1347	45	0.014	700
Phase VIII ⁶	1377	30	0.0093	488
Phase M ⁷	1438	61	0.0190	488

² C-8 Under polymer drive - Phase VI.

³ Well C-6 under polymer drive - Phase VIII.

⁴ Well C-7 and C-8 under polymer drive - Phase VII.

⁵ Well C-8 under polymer drive - Phase VII.

⁶ Well C-6 under polymer drive - Phase M.

⁷ Wells C-7 and C-8 under polymer drive - Phase VIII.

TABLE 7. - Simulation results of micellar-polymer flooding
in barrier island deposystem

Simulation run	Clay content			Preflush, days	Maximum effective salinity, meq/mL	Oil recovery, fraction	Adsorption	
	Layer 1	Layer 2	Layer 3				Surfactant, mL/mL PV	Polymer, wt %, PV
1	0	0	0	109	0.075	0.376	0	0
2	¹ 1% M	² 0.5% K	0.5% K+0.1% M	109	0.078	0.305	0.0022	0.0051
3	1% M	0.5% K	0.5% K+0.1% M	183	0.086	0.349	0.0023	0.0051
4	1% M	0.5% K	0.5% K+0.1% M	274	0.093	0.345	0.0021	0.0057
5	5% M	2.5% K	2.5% K+0.5% M	109	0.080	0.205	0.0049	0.0155
6	5% M	2.5% K	2.5% K+0.5% M	183	0.089	0.224	0.0048	0.0152
7	5% M	2.5% K	2.5% K+0.5% M	274	0.099	0.220	0.0040	0.0150
8	10% M	5% K	5% K+1% M	109	0.080	0.168	0.0057	0.0236
9	15% M	7.5% K	7.5% K+1.5% M	109	0.079	0.149	0.0059	0.0294

¹M = montmorillonite.

²K = kaolinite.

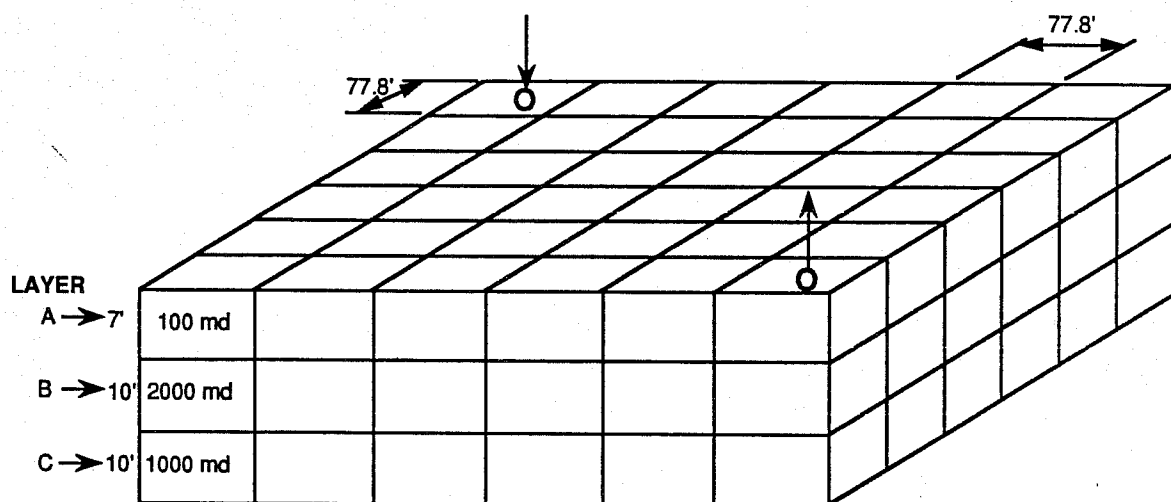


FIGURE 1. - Three-dimensional reservoir model for barrier island deposystem.

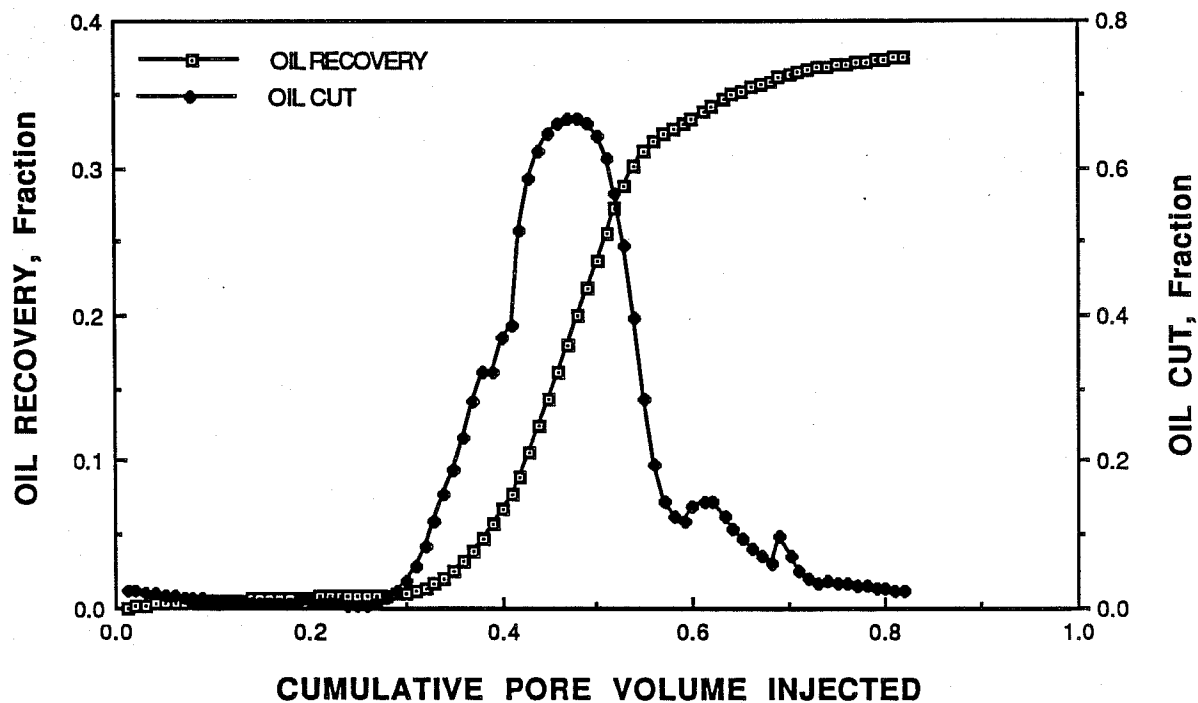


FIGURE 2. - Oil recovery and oil cut from a clay-free barrier island reservoir.

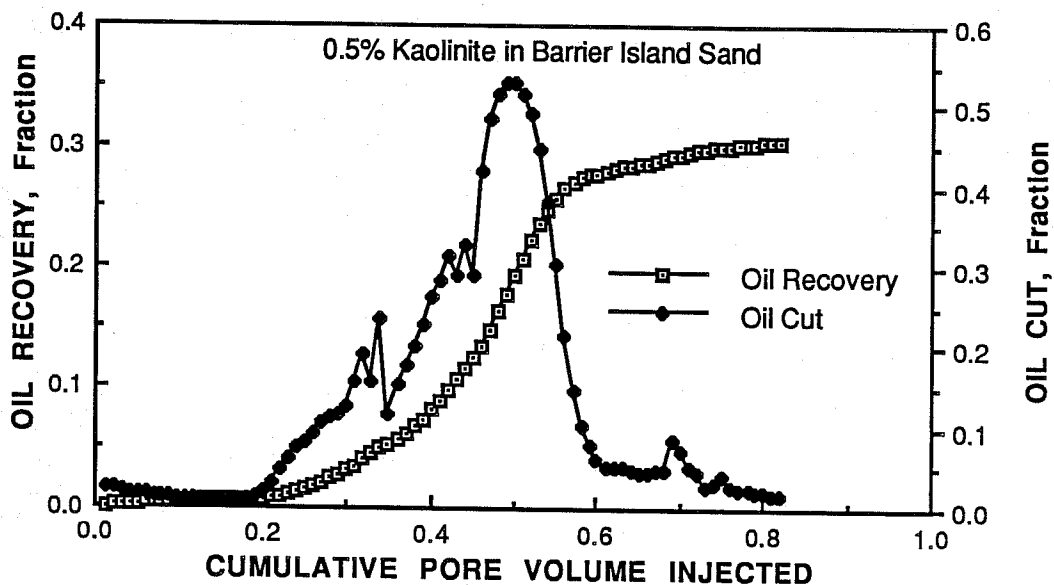


FIGURE 3. - Oil recovery and oil cut from a reservoir containing 0.5% kaolinite in barrier island sand.

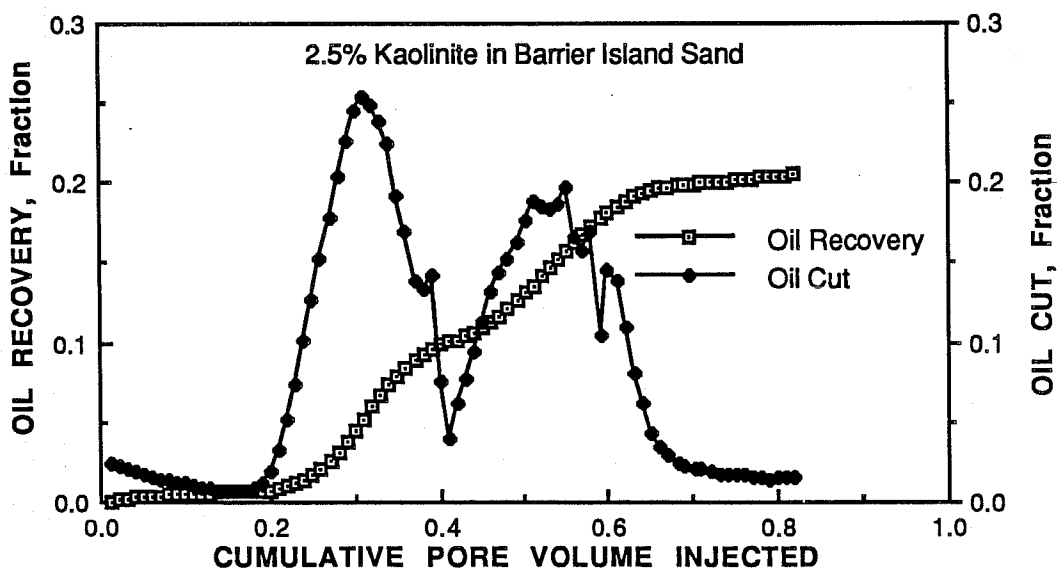


FIGURE 4. - Oil recovery and oil cut from a reservoir containing 2.5% kaolinite in barrier island sand.

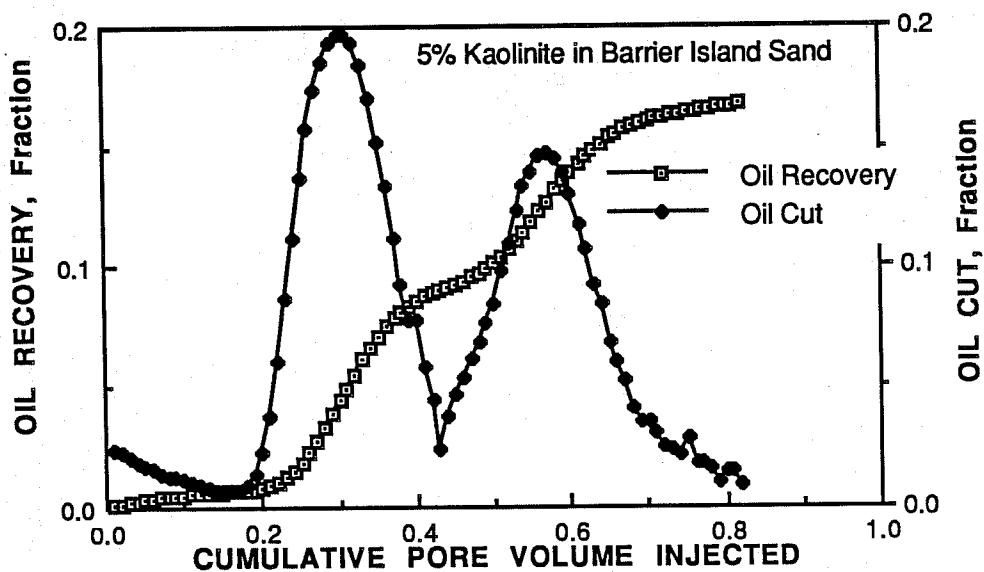


FIGURE 5. - Oil recovery and oil cut from a reservoir containing 5% kaolinite in barrier island sand.

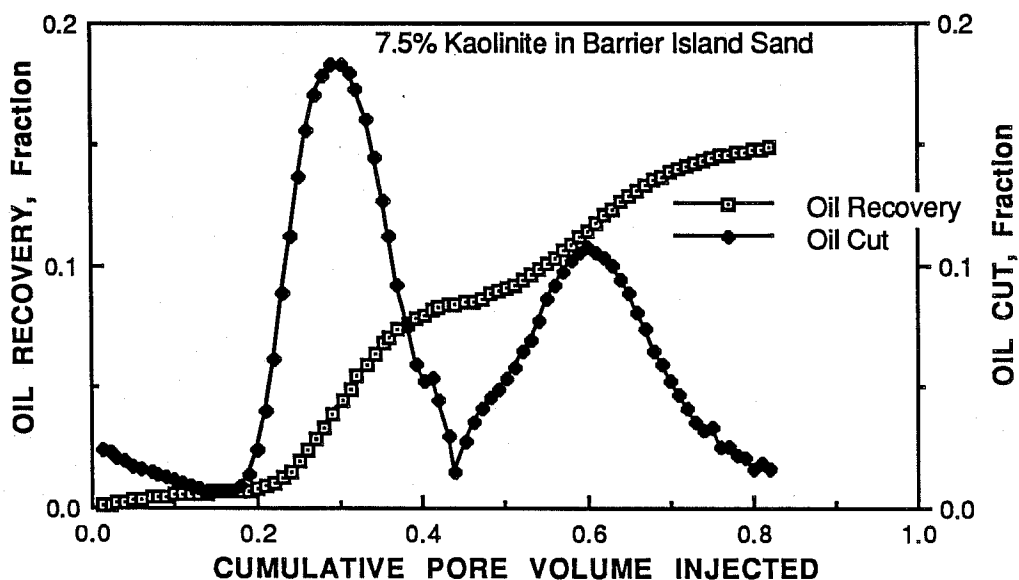


FIGURE 6. - Oil recovery and oil cut from a reservoir containing 7.5% kaolinite in barrier island sand.

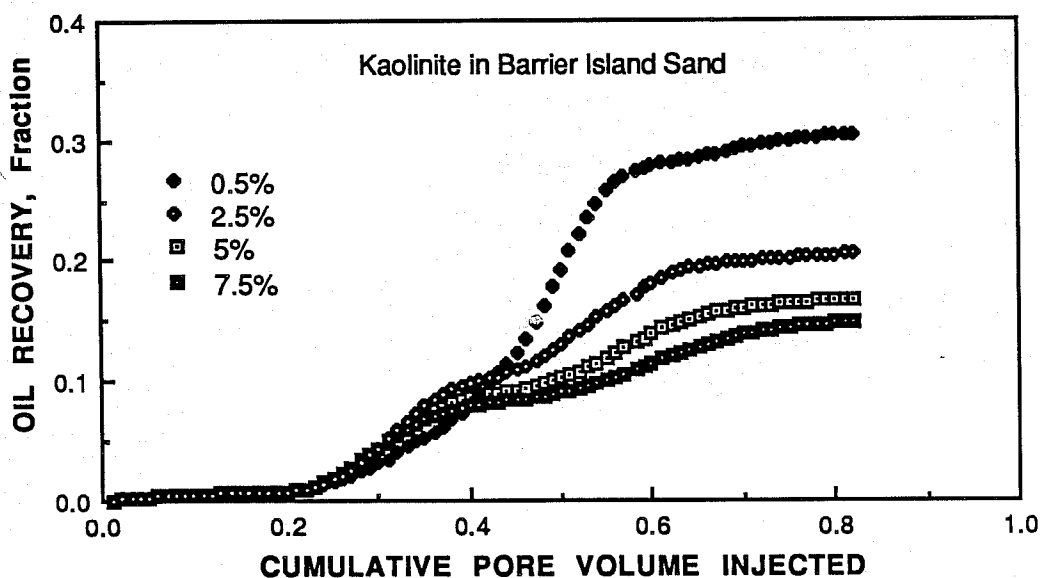


FIGURE 7. - Oil recovery from a barrier island reservoir containing various amount of clay.

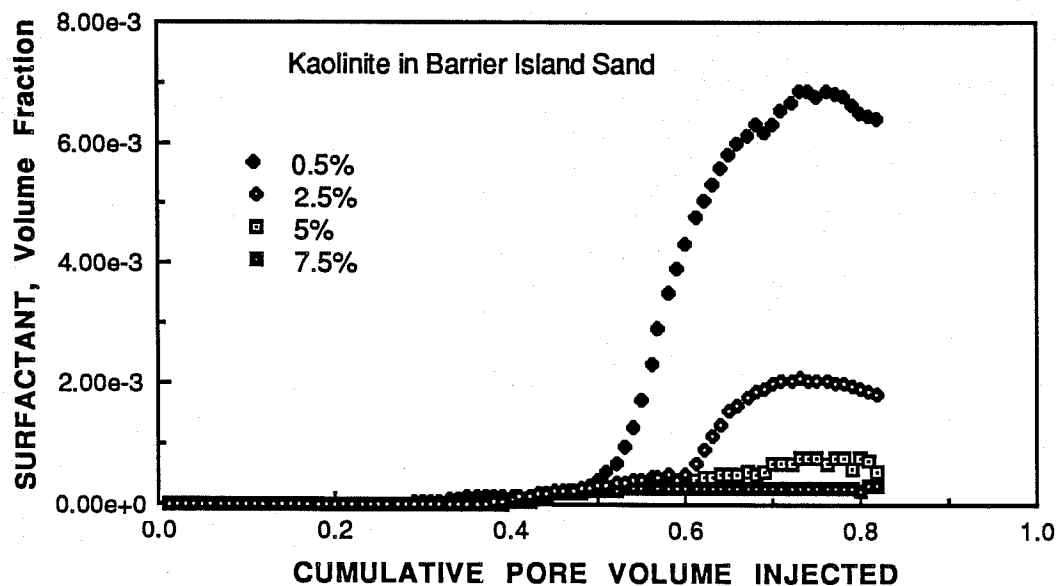


FIGURE 8. - Surfactant profile in aqueous phase from a barrier island reservoir containing various amount of clay.

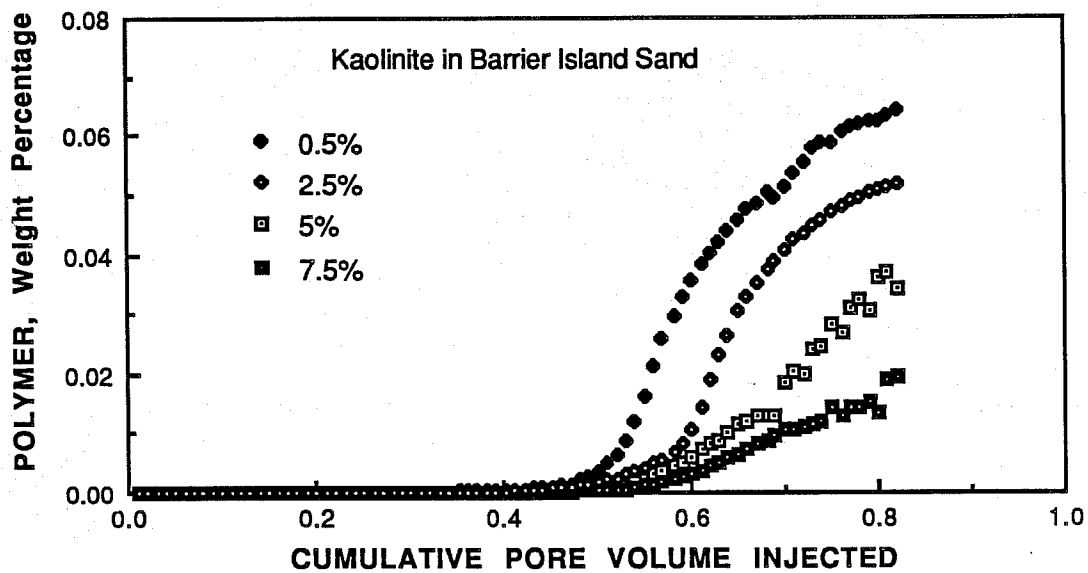


FIGURE 9. Polymer profile from a barrier island reservoir containing various amount of clay.

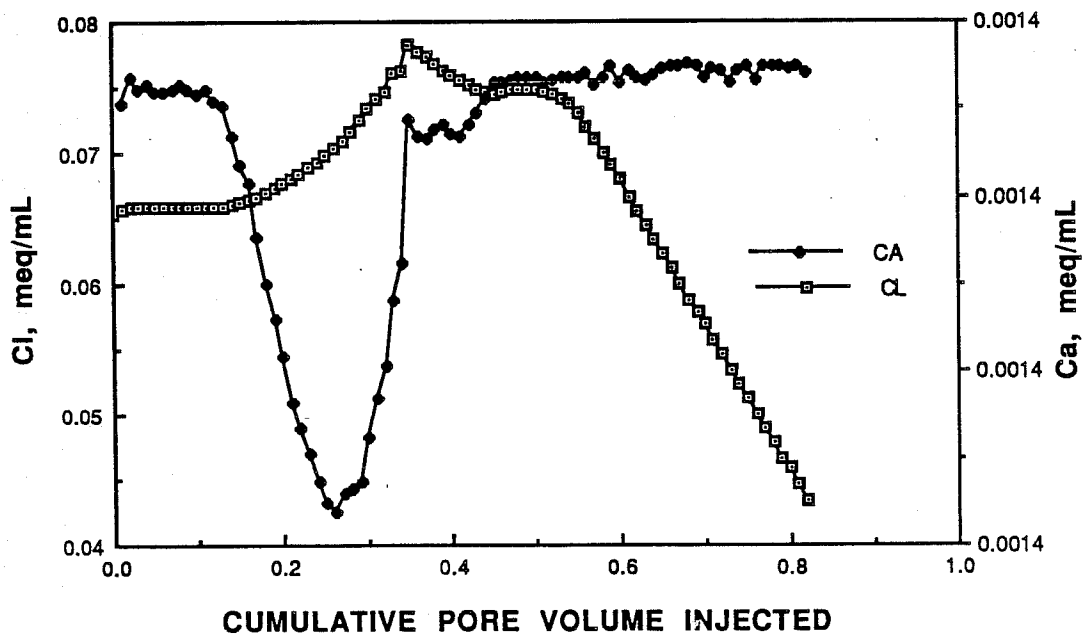


FIGURE 10. - Chloride and calcium profile from a barrier island reservoir containing 0.5% kaolinite in barrier island sand.

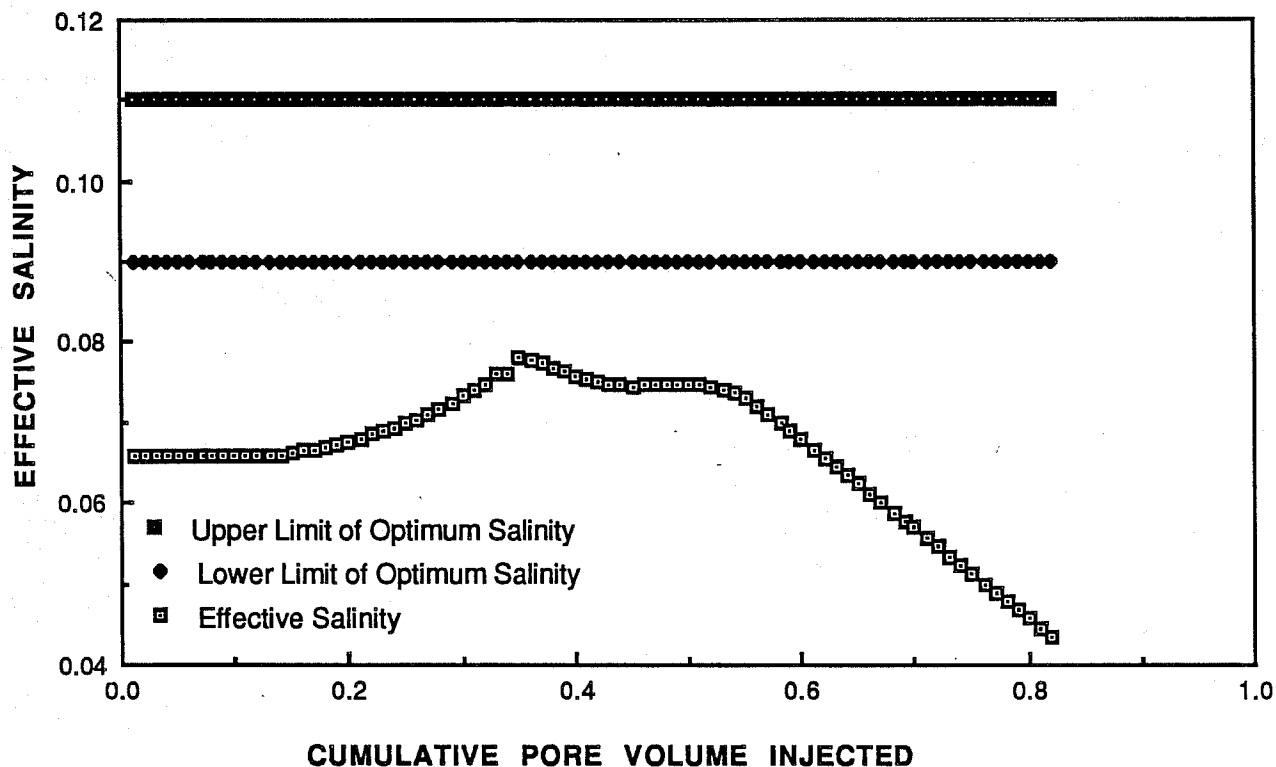


FIGURE 11. - Profile of effective salinity from a barrier island reservoir containing 0.5% kaolinite in barrier island sand.

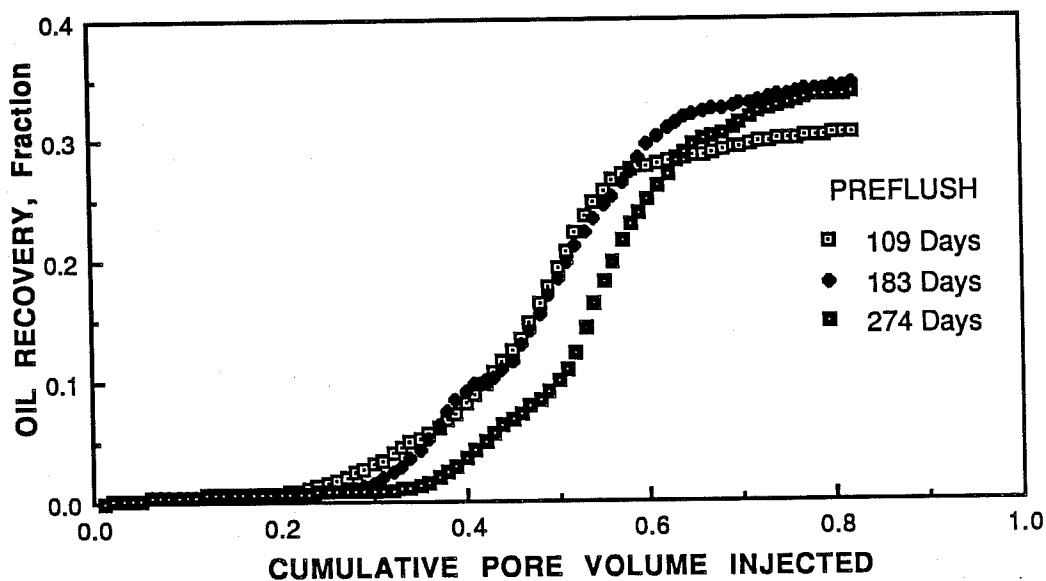


FIGURE 12. - Effect of preflush period on oil recovery from a reservoir containing 0.5% kaolinite in barrier island sand.

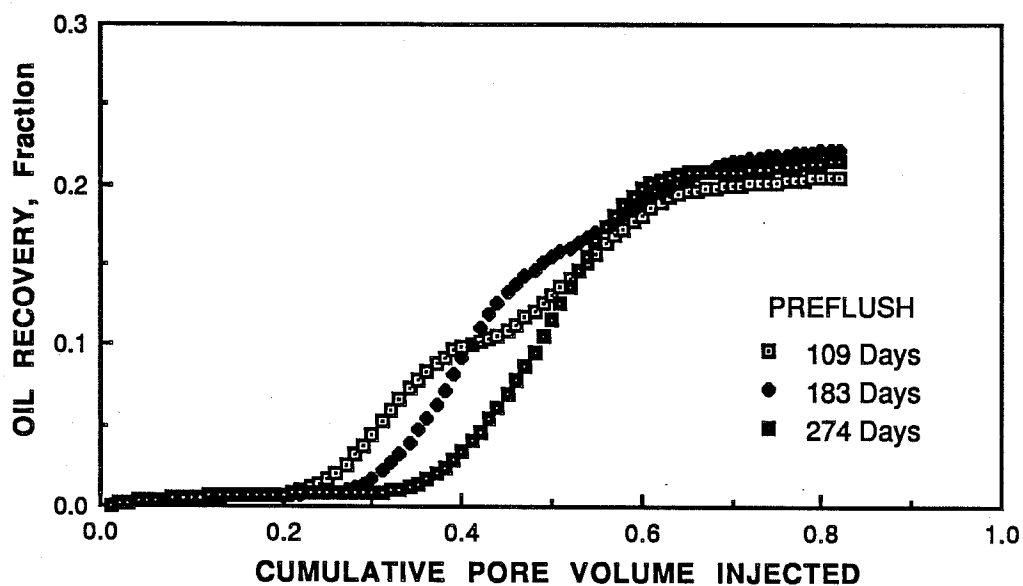


FIGURE 13. - Effect of preflush period on oil recovery from reservoir containing 2.5% kaolinite in barrier island sand.